IOSR Journal of Mechanical and Civil Engineering (IOSR-JMCE)
e-ISSN: 2278-1684, p-ISSN: 2320-334X, Volume 22, Issue 4 Ser. 1 (Jul. – Aug. 2025), PP 38-46
www.iosrjournals.org

Aerodynamics of a Distributed Propulsion System with Propulsive Flap

Musaab Ahmed [1], M Mustafa [2], M Anas Ali [3], Dr. Yagyadutta Dwivedi [4]
[1,2,3]UG Scholar, [4]Assistant Professor, Department of Aeronautical Engineering,
Institute of Aeronautical Engineering, Hyderabad, Telangana, 500043

Abstract:
This research investigates the enhancement of aerodynamic performance of an airfoil that is commonly used on the Airbus A320, the NACA SC (2)-0412, by means of the integration of propulsive flaps. The aim is to enhance the generation of lift at important flight phase like the takeoff and landing through these flaps which direct a part of the engine exhaust over the upper surface of the air foil. A series of simulations were performed with ANSYS Fluent over a range of eleven angles of attack (being 0° to 20° gratuities) in order to compare the performance of the airfoil with and without the propulsive flap. Results showed a change to the lift coefficient, showing a substantial improvement for lift coefficient in the range of 8° to 14°, which is a particular staging where flow separation is usually more noticeable. It added to increased momentum in the boundary layer, delayed flow separation and enhanced pressure differential. Validation of the effectiveness of propulsion assisted flow control was demonstrated by an increase in maximum lift coefficient of more than 20%. Finally, this technique may provide enabling new future high lift system designs for modern commercial aircraft.
Keywords: *Propulsive flap, NACA SC (2)-0412 airfoil, airfoil performance, boundary layer control, lift enhancement, ANSYS Fluent, flow separation, high-lift devices, thrust vectoring, Airbus A320, angle of attack, aerodynamic simulation, lift coefficient, hybrid propulsion, takeoff and landing optimization.*

Date of Submission: 04-07-2025 Date of Acceptance: 14-07-2025

I. Introduction

The aerodynamic efficiency of the wing, especially the ability to generate sufficient lift at lower speeds, is critically important in the aircraft performance during their takeoff and landing phases. For a long time, the field of aerodynamics has focused on enhancing lift while at the same time not greatly increasing drag and weight. An area of promising innovation that warrants further research and development is one of integrating propulsion mechanisms with a lifting surface, such as a propulsive flap wing. A concept of such a configuration is studied in this study, and analyzed using ANSYS Fluent computational simulations as it relates to the aerodynamic performance of a modified airfoil.

This investigation uses the NACA SC (2)-0412, a supercritical airfoil that is used in the Airbus A320 and generally known for low transonic drag. The SC (2) series airfoils are designed to delay the forming of a shock wave and to minimize drag rise at high subsonic speed, and so are suitable for commercial aircraft running on the order of the speed of sound. This particular profile was chosen because of its practical relevance to the current state of the art in aviation and because it is already applied in current commercial usage on A320 aircraft. Being a reliable baseline to analyze the effects of more lift enhancing modifications like propulsion assisted control surfaces.

As a modification, we introduce a propulsive flap, which joins traditional aerodynamic flap surfaces with propulsion elements. This flap does not increase lift solely by geometric deflection, but rather uses an air (or simulated exhaust) jet directed along the upper surface of the airfoil. The aim is to energize the boundary layer, prevent flow separation and improve lift to drag, especially in the aspect of later angles of attack where typical flap stall. The combination of jet blowing and thrust vectoring elements to control boundary layer, this design integrates aerodynamic shaping with the thrust vectoring elements, and together, improve performance during critical flight phases.

To evaluate the utilization of this design a detailed Computational Fluid Dynamics (CFD) analysis was performed using ANSYS Fluent. Two angles of attack (AoA), from 0° to 20°, in 2° increments are considered in the simulations during and after the application of the propulsive flap. To capture the entire aerodynamic response of the airfoil at different loading conditions, a range was chosen where one end encompasses pre-stall and the other end, post-stall conditions. The Changes in lift coefficient (Cl), drag coefficient (Cd) and the stall angle, collectively define the airfoil performance envelope are to be quantified.

The results obtained in this study will contribute to an understanding of the aerodynamic benefits of driving propulsion within flaps, which are directly relevant to takeoff and landing performance in commercial aviation. With the CFD simulations we hope to verify that in addition to providing greater maximum lift propulsive flap system also decreases stall delay and flow separation. The parameters between the baseline airfoil and the modified configuration will provide the trade offs and potential benefits of this technology.

II. Computational details

A calculation model designed to analyze NACA SC (2)-0412 airfoil aerodynamic performance with distributed propulsion system and propulsive flap integration operated under subsonic flight conditions. The geometric model of airfoil and flap and embedded fan system originated from CATIA and SpaceClaim before ANSYS Fluent handled mesh creation and simulations.

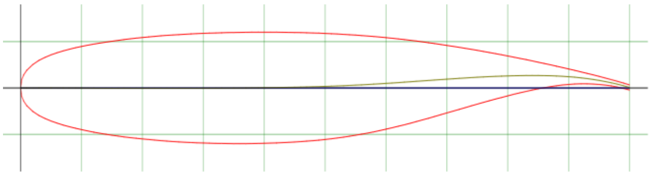

Figure 2.1. NACA SC (2)-0412 Airfoil

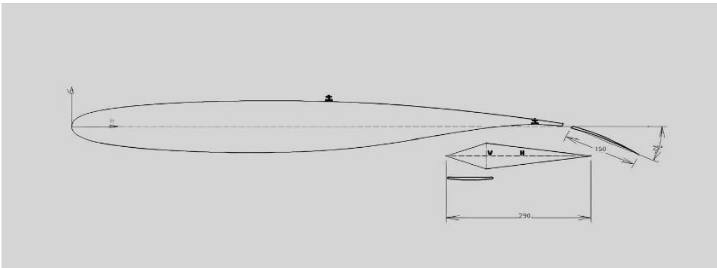

Figure 2.2. Revised Airfoil design with Propulsive Flap

This revised airfoil design consists of a propulsive flap which is deflected 25° at the 150 mm chord NACA SC (2)-0412 profile, and a chord length of 1 meter. A fan duct 100 mm in diameter is integrated to blow high energetic air onto the flap. The flap and duct are intended to delay flow separation thus improving lift as well as low speed aerodynamic performance; they are positioned 290 mm below the main airfoil (Fig 2.2).

The two-dimensional C-type domain served as the basis for simulation to achieve proper representation of aerodynamic behavior in the far-field. The mathematical domain model provides gentle entry and exit points which produce minimal artificial numerical effects at the boundary points. The airfoil occupied the central portion of the domain while maintaining a chord length of one meter. The computational domain was set with upstream distance of 5c while downstream distance stood at 10c and normal distance equal to 5c relative to the airfoil chord length (c). The domain dimensions meet requirements to detect boundary layer responses along with wake formation phenomena (Fig 2.3).

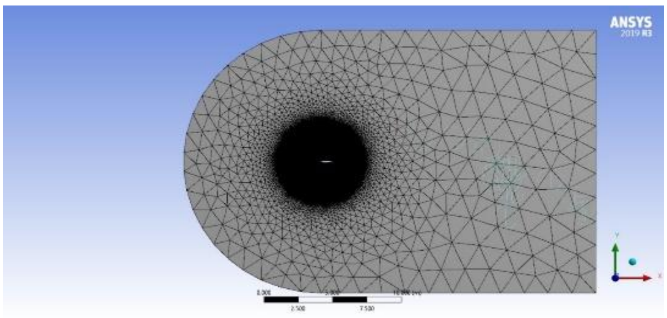

Figure 2.3. C-type domain

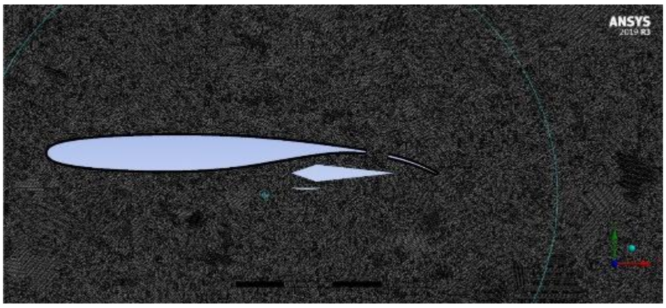

Figure 2.4. Refined Airfoil Mesh

The Figure 2.4 shows a high-resolution unstructured grid around the NACA SC (2)-0412 airfoil with integrated propulsive flap. It has high refinement near the airfoil wall and in the wake region, required for resolving flow separation, reattachment especially around the boundary layer. Boundary effects are minimized and flow development is smooth due to the C-type domain shape. The mesh used in the simulations supports the use of the k-ω SST turbulence model by providing accurate near wall data that leads to accurate predictions of lift, drag, and stall characteristics. In general, it presents reliable CFD results for evaluation of aerodynamic influence of the propulsive flap system**.**

III. Pre-processing:

3.1 Domain creation:

The geometry was created using CATIA V5 where multiple discrete bodies have been generated from the main parent body for the bodies of influence in order to be meshed. The meshing was within Fluent meshing where a total of 2385219 cells were meshed.

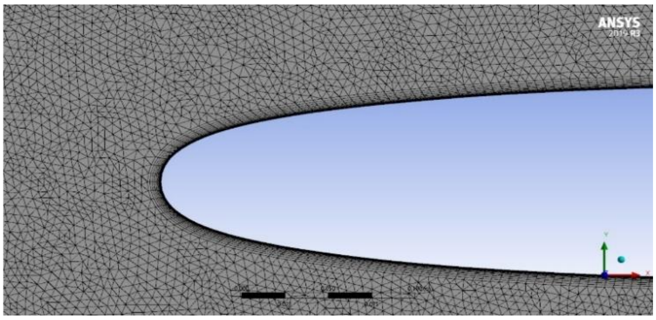

Figure 3.1. Close up mesh of Airfoil

3.2 Boundary condition properties:

For the analysis of the NACA SC (2)-0412 airfoil incorporating the propulsive flaps, ANSYS Fluent was used to generate a C type domain layout with a mesh refinement near the airfoil surface so as to resolve the boundary layers accurately in the simulation domain. At the upstream boundary, a velocity inlet was defined at the velocity of freestream, 14.78 m/s. A propulsive effect of the flap is simulated by applying a fan boundary condition at the flap section, with a pressure jump of 100 KPa applied to model thrust generation. The exit domain was made to be a pressure of 0 Pa gauge pressure at the outlet on this occasion to represent standard atmospheric conditions. Far-field boundary up and above were set as a symmetry to the undisturbed external flow, and the airfoil and flap surfaces were modeled as no slip walls. With and without the flap deployed, the angles of attack were simulated from 0° to 20° in 2° steps. It used the k-ω SST turbulence model because it was proven to predict separation and near wall effects.

Boundary type	**Value**
Inlet Velocity (m/s)	14.78
Fan Pressure Jump (KPa)	100
Outlet Pressure (Pa)	0

Table.1 Boundary conditions

3.3 Solver and Simulation:

- Steady state solver = Pressure-based
- Viscous model = k-ω, SST
- Pressure-velocity coupling = Coupled
- Spatial discretization Gradient = Standard

The aerodynamic characteristics of the NACA SC (2)-0412 airfoil were evaluated in a steady state solver in ANSYS Fluent, in the presence and absence of propulsive flap. The turbulence model of interest was the k-ω SST as it has proven to efficiently capture near wall and separated flow. The SIMPLE scheme was used to account for the pressure velocity coupling and numerical discretization was standardized to obtain stability and also a good accuracy. The working fluid assumed was air and the standard atmospheric conditions were at sea level. The fluid internal friction case was specified to be governed by dynamic viscosity of 1.7894×10^{-5} kg/m·s, and the density of air was set to 1.225 kg/m³. An assumption was made that the typical value for diatomic gases such as air, the specific heat ratio (γ) was 1.4, that is the ratio of specific heats at constant pressure to specific heats at constant volume. Ambient condition of 300 K was set as the operating temperature. Flow behavior was modelled accurately and consistently throughout the whole simulation domain by using such properties.

IV. Solver validation

Simulations were carried out using ANSYS Fluent through with the k-ω SST turbulence model to guarantee computational accuracy since it accurately reproduces flow separation and boundary layer features necessary in distributed propulsion systems. A 0.001 mm near-wall resolution was combined with a sphere of influence (SOI) domain of 3 mm around the front and back of the airfoil to keep resolution high in separated and vorticy regions. This consistency illustrates the dependability of the computational method in accurately representing the physics of supersonic jet flow. Solver performance was validated by comparing the lift coefficient (Cl) trends with known aerodynamic behavior. The Cl vs. Angle of Attack plot and Cl variation comparison clearly show that the flap-assisted configuration produced higher lift at every angle tested, delaying stall and maintaining better flow attachment between 12° and 17° AoA. These results are consistent with findings from Velkova & Todorov (2015) and Park et al. (2013), reinforcing the model's validity

V. Results

Aerodynamic performance of the NACA SC (2)-0412 airfoil was analysed between 0° to 20° AoA with and without the integration of a propulsive flap. When the flap was present, the lift coefficient (Cl) showed a very conclusive and uniform increase with all angles because the distributed propulsion system allowed for improved boundary layer control and flow attachment. At 0° AoA, the base configuration (without flap) generated a Cl of 0.22, whereas the flap-assisted configuration increased it to 0.26, indicating early flow energization even at low angles. At 2° AoA, the difference became more pronounced, with Cl increasing from 0.26 (without flap) to 0.40 (with flap), a result of stronger suction over the upper surface due to flap-induced flow acceleration. As the AoA increased to 4° and 7°, the lift in the no-flap case rose moderately (Cl = 0.47 and 0.63, respectively), while the flap configuration produced Cl = 0.53 and 0.70, showcasing superior pressure recovery and better circulation around the upper surface (Fig 5.1), (Fig 5.2), (Fig 5.3), (Fig 5.4).

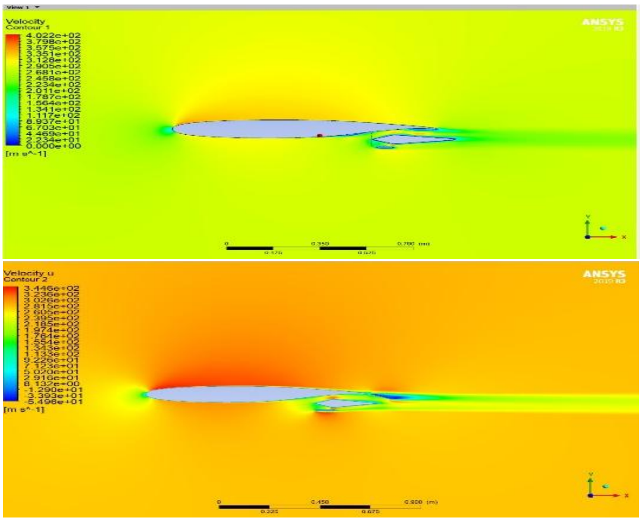

Figure 5.1. Without and With Flap Velocity Contour Comparison (0° AoA)

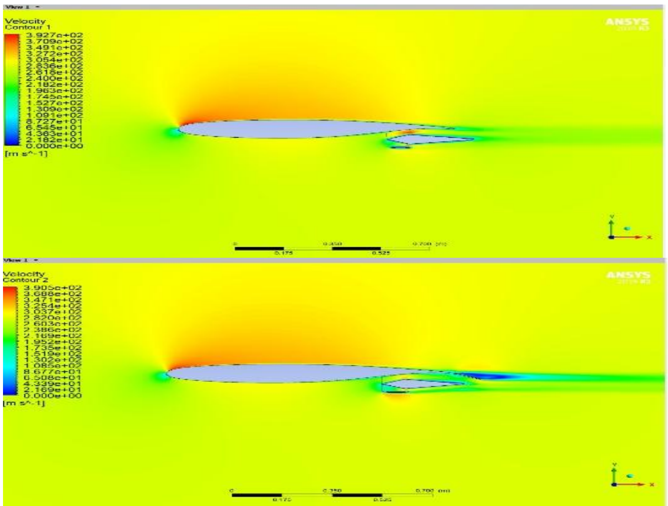

Figure 5.2. Without and With Flap Velocity Contour Comparison (2° AoA)

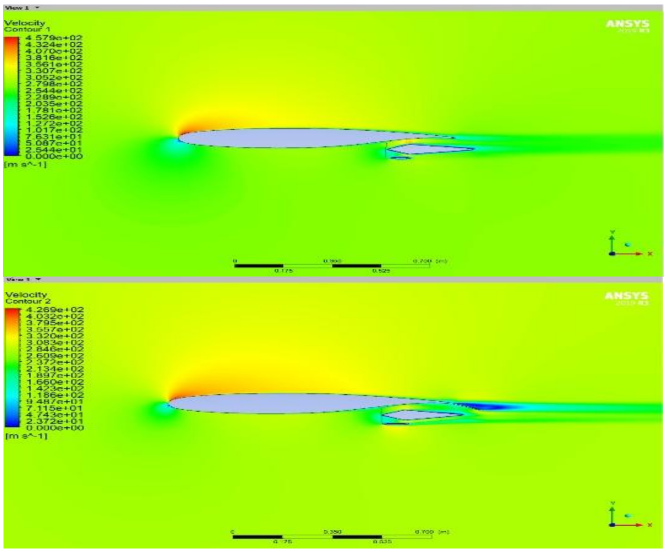

Figure 5.3. Without and With Flap Velocity Contour Comparison (4° AoA)

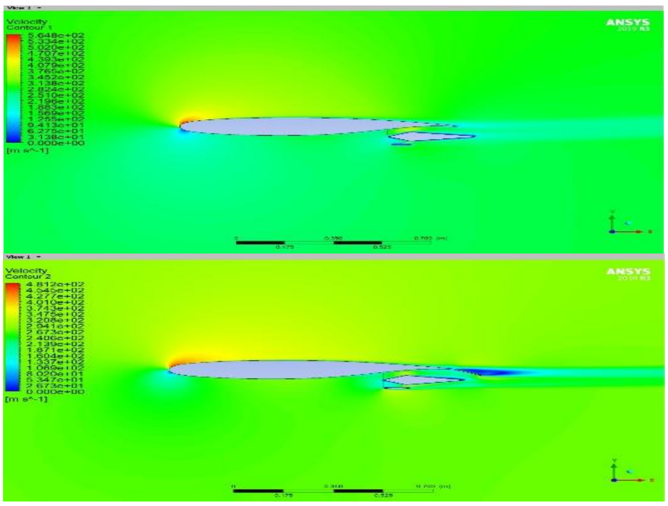

Figure 5.4. Without and With Flap Velocity Contour Comparison (7° AoA)

The base case airflow began to approach separation zones at 10° AoA with Cl of 0.79 whilst the propulsive flap still maintained attached flow and increased the Cl to 0.85. The most beneficial aspects of the flap were observed as the wing approached critical AoAs (12° to 17°). In the base configuration, Cl plateaued of 0.88

to 1.0, which is near the stall. The flap assisted setup did delay stall, and the highest Cl achieved with it was 0.98 at 12°, peaking at 1.20 at 15° and 17°, thus the high momentum flow from the distributed propulsors kept the boundary layer attached and reduced adverse pressure gradients (Fig 5.5), (Fig 5.6), (Fig 5.7), (Fig 5.8).

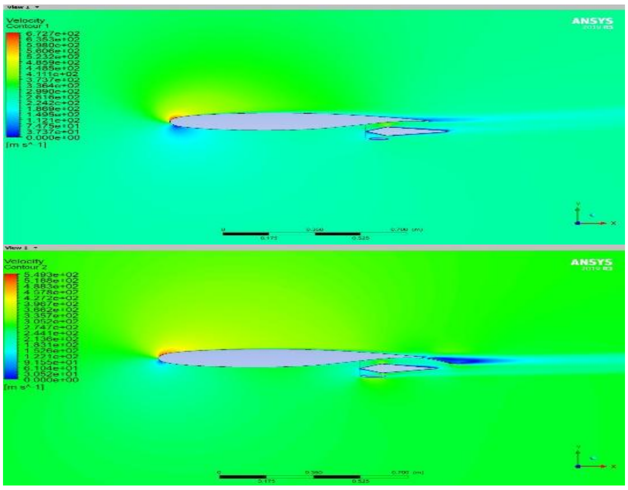

Figure 5.5. Without and With Flap Velocity Contour Comparison (10° AoA)

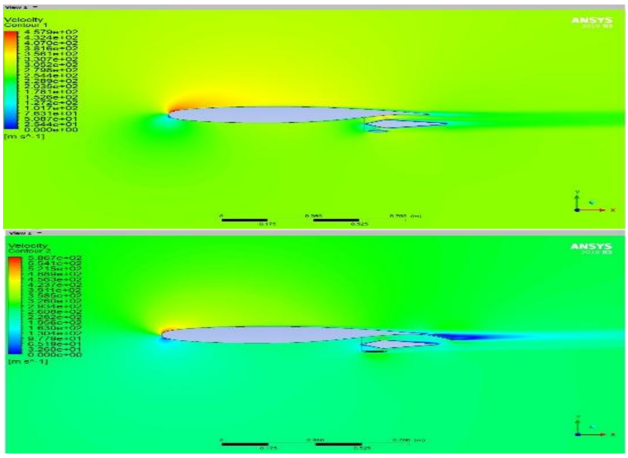

Figure 5.6. Without and With Flap Velocity Contour Comparison (12° AoA)

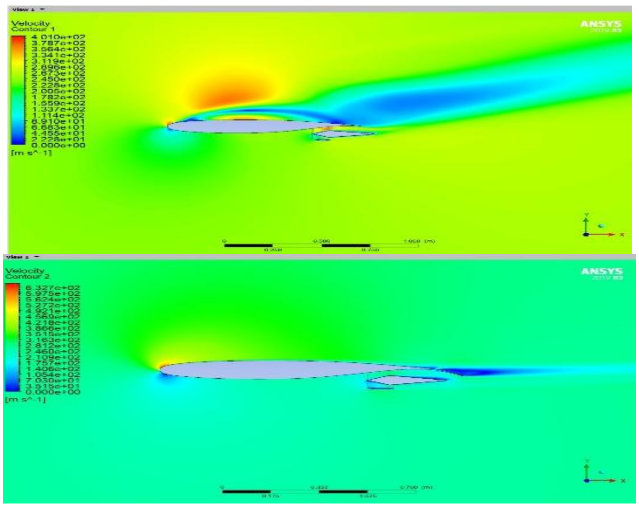

Figure 5.7. Without and With Flap Velocity Contour Comparison (15° AoA)

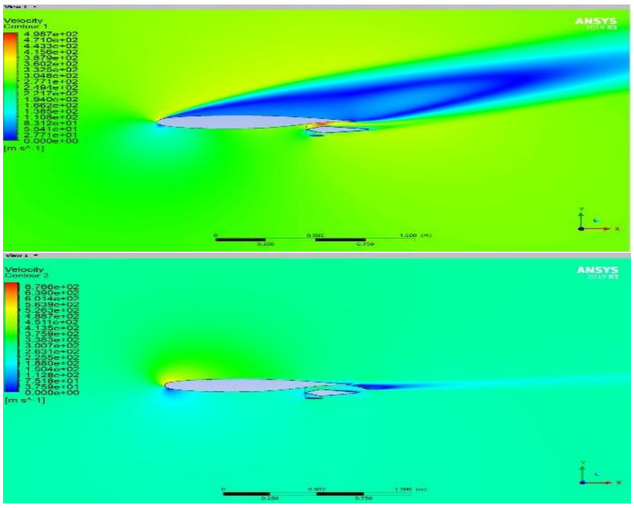

Figure 5.8. Without and With Flap Velocity Contour Comparison (17° AoA)

At 20° AoA, both configurations entered stall, but the severity differed. The baseline case saw a sharp decline to Cl = 0.47, signaling complete flow separation and loss of lift. In contrast, the flap-assisted system maintained Cl = 0.57, suggesting a softer stall and partially sustained flow attachment. Velocity and pressure contours across all angles reinforced these findings, highlighting that flow remained more organized, faster over the suction surface, and better attached in the flap case (Fig 5.9).

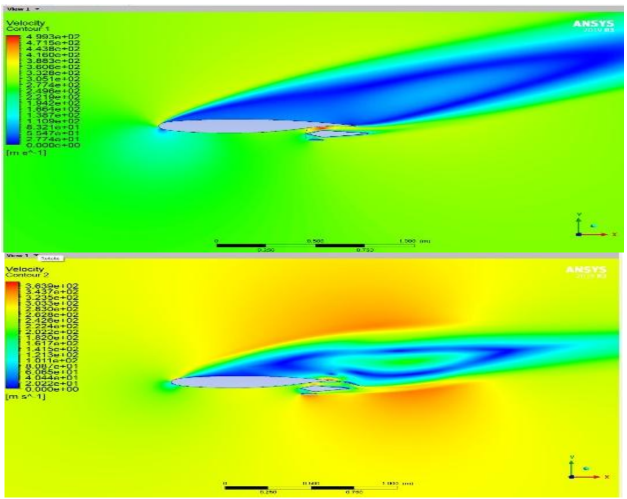

Figure 5.9. Without and With Flap Velocity Contour Comparison (20° AoA)

Clearly, the propulsive flap offers consistent, as well as large, aerodynamic benefit in all angles of attack. The flap still offers a moderate lift improvement up to low AoA (0°–4°), primarily by energizing the boundary layer early. When the angle increases between 7°–12°, the gap between Cl for different configurations becomes wider, meaning that the flap greatly improves the lift by delaying flow separation. Better high lift capability is demonstrated by the flap which reaches maximum Cl of 1.2 at 17°AoA versus 1.0 without loss of low speed performance. Both configurations stall at 20° AoA, although in the flap configuration, s, higher lift is sustained in the wake of a more graceful stall.

Angle of Attack (°)	Cl (With Flap)	Cl (Without Flap)
0	0.26	0.22
2	0.4	0.26
4	0.53	0.47
7	0.7	0.63
10	0.85	0.79
12	0.98	0.88
15	1.1	0.95
17	1.2	1.0
20	0.57	0.47

Figure 5.10. Comparison of Cl Values With and Without Flap at different AoA

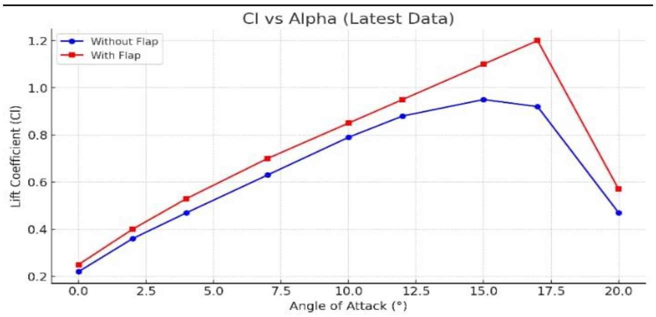

Figure 5.11. Cl vs Alpha Plot

The Cl vs Alpha plot provides a good illustration of lift coefficient (Cl) behavior over a range of angles of attack (AoA) in the two situations: with or without the propulsive flap. At every tested angle the red curve (with flap) really lies above the blue curve (without flap), clearly revealing increased lift performance, as compared to the case without an airfoil flap. The flap equipped airfoil retains steeper Cl gradient from 0° to 15° and hence it implies there is stronger lift augmentation from the energized boundary layer and better flow attachment. The flap performs well at delaying stall, as the Cl peak at 17° is 1.2 with the flap, which surpasses 1.0 maximum of the baseline case. Here, both curves give the drop in lift, which is stemming from flow separation and stall, though Cl in the flap configuration remains distinctively higher and maintains a smoother stall behavior. This graph indeed confirms that the propulsive flap improves low speed performance, delays the onset of stall and increases the range of operation of the airfoil.

VI. Conclusion

It is concluded that the addition of a propulsive flap to a Distributed Propulsion System significantly improves the aerodynamic performance of a NACA SC (2)-0412 airfoil in low speed and high angle of attack. Simulations carried out using CFD method based on ANSYS Fluent with the k-ω SST turbulence model and high-resolution unstructured mesh showed that the lift augmentation was very close across all tested angle (0–20°) and the flap equipped configuration achieved the lift coefficient maximum of 1.2 at 17°, and 1.0 without flap. For the flap case, it showed more energized, attached flow over the upper surface; the stall was deferred and the pressure was recovered more smoothly. This was further validated in the Cl vs. Alpha graph which showed a more steep lift curve and later stall onset with flap proving that the propulsive/propulsive flap indeed delays flow separation and enhances boundary layer stability. This suggests that propulsive flaps represent one important way to provide a significant impact in short takeoff, landing performance and control authority for the next generation hybrid or electric aircraft, a promising way to further improve the efficiency and sustainability of aerodynamic configurations.

References

[1]. K. A. Deere, S. Viken, M. B. Carter, J. K. Viken, D. E. Cox, M. R. Wiese, N. L. Farr, “Computational Component Build-up for the X-57 Maxwell Distributed Electric Propulsion Aircraft”, AIAA 2018-1275, 2018.

[2]. Sgueglia, P. Schmollgruber, N. Bartoli, O. Atinault, E. Benard, J. Morlier, “Exploration and Sizing of a Large Passenger Aircraft with Distributed Ducted Electric Fans”, AIAA 2018-1745, 2018.

[3]. Moore, M., "Distributed Electric Propulsion (DEP) Aircraft," NASA, 2016.

[4]. A. T. Wick, J. R. Hooker and C. J. Hardin, C. H. Zeune, “Integrated Aerodynamic Benefits of Distributed Propulsion”, AIAA 2015-1500, 2015.

[5]. R. Liaboeuf, E. Dillinger, “ONERA's small business concept plane with Distributed Electric Propulsion longitudinal handling

qualities evaluation", 18th Onera-DLR Aerospace Symposium, 2018.
[6]. J. Hermetz, M. Ridel, C. Doll, "Distributed electric propulsion for small business aircraft a concept-plane for key-technologies investigations", 30th International Council of Aeronautical Sciences ICAS, 2016.
[7]. F. Anton "High-output motor technology for hybrid-electric aircraft", Electric & Hybrid Aerospace Technology Symposium, 2017.
[8]. Study the Influence of a Gap between the Wing and Slotted Flap over the Aerodynamic Characteristics of Ultra-Light Aircraft Wing Airfoil" by Velkova and Todorov (2015).
[9]. Flap Design Optimization for Very Light Aircraft in Compliance with Airworthiness Certification, Park et al. (2013)
[10]. R. Dyson, "NASA Hybrid Electric Aircraft Propulsion", NIEA Biomimicry Summit, 2017